Received: 29 September 2015 | Revised: 4 February 2018 | Accepted: 1 June 2018

DOI: 10.1002/rnc.4252

RESEARCH ARTICLE

WILEY

A liquid sphere-inspired physicomimetics approach for multiagent formation control

Xun Wang[1,2] | Xiangke Wang[2] | Daibing Zhang[2] | Lincheng Shen[2]

[1]State Key Laboratory of Intense Pulsed Radiation Simulation and Effect, Northwest Institute of Nuclear Technology, Xian, China

[2]College of Mechatronics and Automation, National University of Defense Technology, Changsha, China

Correspondence
Xiangke Wang, College of Mechatronics and Automation, National University of Defense Technology, Changsha 410073, China.
Email: xkwang@nudt.edu.cn

Funding information
Research Project of the National University of Defense Technology, Grant/Award Number: JC-13-03-02; National Natural Science Foundation of China, Grant/Award Number: 61403406

Summary

A liquid sphere-inspired physicomimetics approach is presented for multiagent formation control. The agents are formulated as a liquid sphere, which is modeled by a virtual spring network. Then, a decentralized controller is obtained for each agent. The stability and convergence are proved. The scalability and flexibility are analyzed. Using the proposed approach, arbitrarily shaped formations can be obtained; and an extra agent can be added to a formation like mixing a drop of liquid into a liquid sphere. By designing extra virtual repulsive forces from obstacles, a formation avoids obstacles like a fluid flowing over obstacles or squeezing through narrow passages. The required number of communication links is N for N agents. The use of physicomimetics makes the approach computationally simple, and the physical meanings of the parameters definite. To illustrate the advantages of the proposed approach, a structural potential function-based approach is selected as the comparative method. Simulation results demonstrate the effectiveness of the liquid sphere-inspired formation control approach.

KEYWORDS

formation control, liquid sphere, multiagent system, obstacle avoidance, physicomimetics

1 | INTRODUCTION

Research on the formation of multiagent systems has attracted growing interest in recent years,[1,2] triggered mainly by the technological advances in control techniques for single vehicles and the explosion in computational and communication capabilities. Research in the field of formation control and coordination for multiagent systems is currently progressing in areas, such as the formation of unmanned aerial vehicles (UAVs),[3] unmanned underwater vehicles,[4] satellites,[5] and spacecraft.[6]

Various control strategies for multiagent formations have been investigated for many years, such as the leader-follower approach,[7-9] virtual structure approach,[10-12] behavior-based approach,[13,14] artificial potential field (APF) approach,[15-18] and motion planning approach.[19] Besides, different approaches for multiagent formation are well reviewed in other works[20-22] from different viewpoints. Among these approaches, APF-based approaches are similar to the work in this paper to some extent. In the work of Fax and Murray,[15] APF was used to design a distributed control law for the coordination of multiple vehicles. The distributed control law for each vehicle did not depend on the state of all other vehicles in the formation. However, it does not guarantee stabilization of the system of multiple vehicles to a unique desired formation. In the work of Olfati-Saber and Murray,[16] a structural potential function (SPF)–based approach was proposed for multivehicle formations. The SPF-based approach imposed a specific structure on a weighted graph associated with the formation of the vehicles, guaranteeing that the multivehicle system converged to a unique desired formation. However, the required

communication links were considerable in the SPF-based approach. In terms of flexibility and scalability, the APF-based approaches could be used to address the problem of transformation and the addition of an extra agent to a formation, but the distributed controllers for all of the corresponding agents need to be reconfigured. Motivated by the aforementioned considerations, we focus on a novel physicomimetics approach for the formation control in this paper.

The concept of "physicomimetics" was first introduced in the work of Spears et al.[23] Physicomimetics is a type of artificial physics. The basic idea originates from natural physics, such as Newton's second law and universal gravitation. They used virtual physics forces to drive a multiagent system to a desired state. The desired state is one that minimizes the system's overall potential energy. In the physicomimetics approach, each agent acts as a molecular dynamic ($F = ma$). Thus, physicomimetics is founded upon solid scientific principles. As an example,[23] formulated vehicle swarms as various regular geometric lattice configurations by modeling the interactive force using virtual physics forces, which is similar to universal gravitation. Such a solid-based physicomimetics approach is suitable for aggregation problems but has less flexibility. Two formal gas models were proposed for multiagent sweeping and obstacle avoidance in the work of Kerr et al.[24] With the gas models, if a container is designed, the gas can eventually diffuse throughout the container until it reaches an asymptotic state. Therefore, gas-based physicomimetics approaches can be used to address coverage problems, such as sweeping[24] and surveillance[25] within a bounded area.

In general, fluids, including both gases and liquids, are able to take the shape of their container and therefore are well suited for obstacle avoidance.[24] Fluids are also capable of squeezing through narrow passages and then resuming full coverage when the passage expands. Different from gases, liquids can take the shape of an ideal sphere due to the intermolecular force and surface tension when there is no gravity, such as in space,[26] so the container is not necessary when we formulate a formation as a liquid. Accordingly, a liquid-based physicomimetics approach is an alternative direction to formulate a flexible formation of a multiagent system.

In this paper, we propose a liquid sphere-inspired physicomimetics approach for multiagent formation control. The multiagent system is formulated as a liquid sphere using a virtual spring network. The virtual intermolecular force is modeled as a virtual spring between each agent and the formation center. The virtual spring force ensures that the agents converge to the desired formation circle. In this direction, the liquid sphere-inspired controller is equivalent to the feedback linearization method combined with the proportion differential (PD) method. The virtual surface tension is modeled as virtual angle springs between adjacent agents. These forces ensure the desired distribution of all the agents on the circle. To prevent oscillations, drag coefficients are added to all the virtual (angle) springs. By regulating the rest lengths and the spring constants of the virtual springs, an arbitrarily shaped formation can be obtained. Moreover, the scalability and flexibility of the approach are evaluated by analyzing the processes of extra agent addition, transformation, and obstacle avoidance. To illustrate the advantages of our approach over the traditional APF-based approach, one of the most cited approaches proposed by Olfati-Saber and Murray[16] is selected as a comparative method.

The main contribution of this paper is the liquid sphere-inspired physicomimetics approach. Using the proposed approach, an arbitrarily shaped formation can be obtained. We can easily add an agent to a formation like mixing a drop of liquid into a liquid sphere. By designing extra virtual repulsive forces, a formation avoids obstacles like fluids flowing over obstacles or squeezing through narrow passages. Furthermore, the liquid sphere-inspired approach is decentralized. The decentralized controller for every agent only depends on its own state and the states of its two neighbors. The decentralized structure can reduce the communication required and limit the complexity of individual agent controllers. Moreover, the approach is founded on solid physical theory and is computationally simple because of its use of artificial physics. The physical meanings of the parameters are definite, which makes it easy to tune in application.

The remainder of the paper is organized as follows. We formulate the problem and give some basic concepts related to the proposed formation control approach in Section 2. The approach, along with the proof of stability and convergence, is presented in Section 3. The arbitrarily shaped formation is further analyzed in Section 4. The extension abilities of the approach, including scalability, formation switching, and obstacle avoidance, are discussed in Section 5. In Section 6, we briefly describe the comparative method proposed by Olfati-Saber and Murray,[16] and then a series of simulation results are presented to verify our approach. Finally, we conclude the paper in Section 7.

2 | PROBLEM FORMULATION AND BASIC CONCEPTS

In this section, we first give our objective and the agent model. Then, we briefly describe the properties of a liquid sphere, from which we obtained the idea of the proposed physicomimetics approach. After that, we present a virtual spring network to formulate a liquid sphere.

2.1 | Objective

In this paper, our motivation is to formulate the formation of a multiagent system as a liquid sphere such that the multiagent system can move as a whole and has some features of liquids, such as the abilities of scalability and obstacle avoidance. With these features, extra agents can be added to a formation like mixing a drop of liquid into a liquid sphere, and the formation can avoid obstacles like fluid flow over obstacles.

2.2 | Agent model

Second-order integral models are used for multiagent systems. For the ith agent A_i ($i = 1, 2, \dots, N$), the second-order integral model is given by

$$\dot{\mathbf{p}}_i = \mathbf{v}_i, \dot{\mathbf{v}}_i = \mathbf{a}_i, \tag{1}$$

where $\mathbf{p}_i = [x_i, y_i]'$, $\mathbf{v}_i = [v_{ix}, v_{iy}]'$, and $\mathbf{a}_i = [a_{ix}, a_{iy}]'$ denote the position, velocity, and acceleration of A_i. Based on the second-order integral models, the agents are governed by Newton's law ($F_i = m_i a_i$), where m_i, a_i, and F_i are the mass, acceleration, and total force acting on A_i.

The structures of leader-follower and virtual leader are popular for the problem of multiagent formation. Normally, the states of the (virtual) leader are known to all the followers. Some recent work has addressed the problem of when only a few agents know the states of the leader.[27] This idea can be utilized to improve the structures of the traditional leader-follower and virtual leader approaches. Meanwhile, in this paper, to focus on the idea of the liquid sphere-inspired physicomimetics, the following assumption is noted before proceeding further.

Assumption 1. The multiagent system follows a virtual target, and the states of the virtual target are known to all agents. Every agent knows its location and velocity and is able to communicate with two agents predetermined in the formation.

By the assumption, each agent has 2 neighbors to communicate with. The structure is designed to apply the structure of the liquid sphere modeled by a virtual spring network. Besides, it implies that all the neighbors are within the communication range of each other and practical communication problems such as delay and loss are beyond the scope of this paper.

2.3 | Liquid sphere

Without gravity and disturbances, a liquid sphere takes the shape of a perfect sphere due to the intermolecular force and surface tension.[26] The molecules on the surface of the liquid sphere will be uniformly distributed due to the surface tension. Many liquid sphere experiments have been conducted in space by astronauts, as shown in Figure 1. From the perspective of energy minimization, the sphere is the minimal potential energy configuration of the molecules. Potential energy is defined by the positions of the molecules relative to each other and the forces between them. The system loses potential energy by transforming it into thermal energy.

2.4 | Virtual spring network

In engineering and physics, a spring network is a collection of point masses connected by a series of springs, roughly in the shape of the desired object. This generalizes Hooke's law to higher dimensions. With the linear spring assumption,

FIGURE 1 Liquid sphere in space experiments [Colour figure can be viewed at wileyonlinelibrary.com]

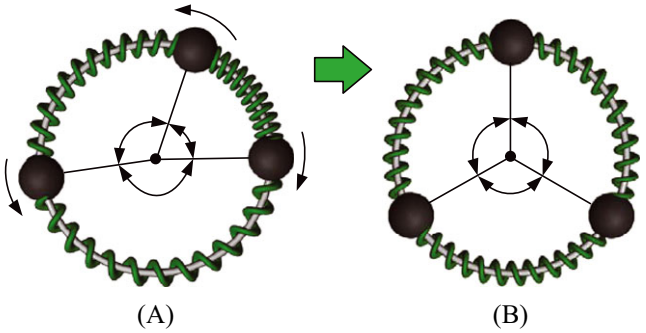

FIGURE 2 Spring network in a circular shape. A, Nonequilibrium state; B, Equilibrium state [Colour figure can be viewed at wileyonlinelibrary.com]

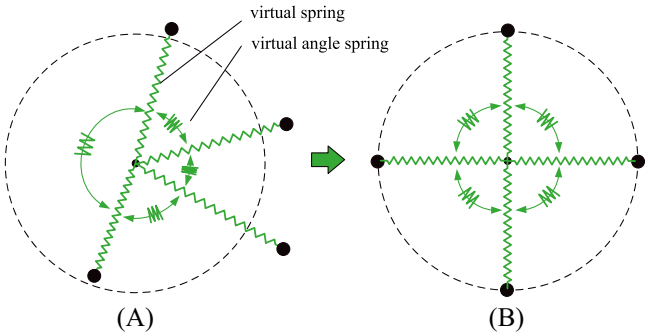

FIGURE 3 Virtual spring network to simulate liquid sphere. A, Nonequilibrium state; B, Equilibrium state [Colour figure can be viewed at wileyonlinelibrary.com]

a spring network, as shown in Figure 2, can be cast as a system of linear equations or equivalently as an energy minimization problem, which can be used to simplify and formulate the surface tension of a liquid sphere.

In the circular spring network in Figure 2, the force of the spring along the circle is similar to the "angle spring force," which ensures equal angle clearance between adjacent agents. Here, we introduce the concept of a virtual angle spring. A virtual angle spring connects the two edges of an angle, as in Figure 2, and has three basic features.

1. The angle spring exerts a moment of force on the virtual center through the connected edges.
2. The rest angle is 0, which means the angle spring is always stretched.
3. The torque exerted by the angle spring is proportional to the angle, which means the torque $\tau = k_\theta \theta$, where k_θ is the angle spring constant and θ is the angle.

Then, the dynamics of a liquid sphere can be simplified and modeled by a virtual spring network in which the intermolecular force is modeled by a simple virtual spring between the center and each agent and the surface tension is modeled by a virtual angle spring between adjacent agents. The designed virtual spring network model is shown in Figure 3. It is worthwhile to note that the use of virtual springs and virtual angle springs in the radial and angle directions makes the virtual spring network model decoupled in the two orthogonal directions.

The word "virtual" here means that the spring force (or torque) is a type of artificial force (or torque) that does not exist in real systems. We also use the word "virtual" to indicate that, although we are motivated by natural physical forces, we are not restricted to them. The virtual force may have some features that are beyond the "actual" physics. For example, the rest angle of the virtual angle spring is 0. Although the forces are virtual, the agents act as if they were real.

3 | THE LIQUID SPHERE-INSPIRED FORMATION CONTROL APPROACH

In the formation of a multiagent system, a formation center is needed to formulate the total formation with the conception of the virtual spring network, as shown in Figure 3. A virtual center is designed as the formation center. When the formation is required to move, the virtual center can be designed to track the virtual target in Assumption 1, which acts as a virtual leader.

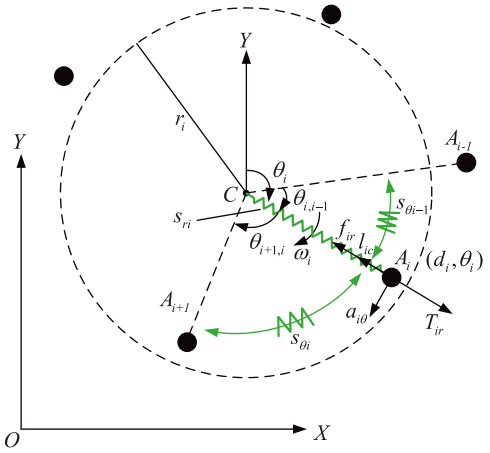

FIGURE 4 The diagram of the liquid sphere-inspired formation controller for A_i [Colour figure can be viewed at wileyonlinelibrary.com]

For a multiagent system with N agents, we define a point C as the virtual formation center so that any ray from C goes through no more than one agent. As shown in Figure 4, $O-XY$ denotes the local world coordinates. We define the polar coordinates $C-d\theta$, where the radial coordinate d is the distance from C and θ denotes the polar angle from the polar axis Y in the clockwise direction. By labeling the agents according to the initial θ of each agent, we have A_i $(i = 1, 2, \dots, N)$ with $\theta_i < \theta_j$ for $1 \leqslant i < j \leqslant N$. Then, A_{i-1} and A_{i+1} are defined as the two neighbors of A_i $(i = 1, 2, \dots, N)$, where $A_0 = A_N$ and $A_{N+1} = A_1$. Analogously, we have $\alpha_0 = \alpha_N$ and $\alpha_{N+1} = \alpha_1$ for any variable α in the reminder. According to Assumption 1, every agent knows the states of C and communicates with its two neighbors.

According to the virtual spring network model, as shown in Figure 3, there are three virtual (angle) springs related to A_i, ie, the virtual spring S_{ri} connecting A_i to the virtual center C, the virtual angle spring $S_{\theta i-1}$ between CA_{i-1} and CA_i, and $S_{\theta i}$ between CA_i and CA_{i+1}. Then, the dynamics of the virtual spring network model can be decoupled and divided into radius direction and polar angle direction for each agent.

In the radius direction, the rest length, spring constant, and drag coefficient of S_{ri} are r_i, k_{vri}, and c_{vri}, respectively. Then, the resultant radial force in the radius direction is given by

$$F_{ir} = m_i a_{ir} = T_{ir} - f_{ir} - l_{ic} \tag{2}$$

$$\begin{cases} T_{ir} = k_{vri}(r_i - d_i) \\ f_{ir} = c_{vri}\dot{d}_i \\ l_{ic} = m_i d_i \omega_i^2, \end{cases} \tag{3}$$

where a_{ir} is the radial acceleration of A_i. T_{ir} and f_{ir} denote the elasticity and resistance in the radius direction. l_{ic} is the centripetal force. ω_i is the angle rate of CA_i in the polar angle direction.

Substituting (3) into (2), we obtain the radial acceleration

$$a_{ir} = \frac{k_{vri}}{m_i}(r_i - d_i) - \frac{c_{vri}}{m_i}\dot{d}_i - d_i\omega_i^2. \tag{4}$$

In the polar angle direction, the rest angle and spring constant of $S_{\theta i}$ are 0 and $k_{v\theta i}$, and $c_{v\theta i}$ is the angle drag coefficient of CA_i. Then, the resultant torque of CA_i on C can be given by

$$\tau_i = I_i\dot{\omega}_i = \tau_{i+1,i} - \tau_{i,i-1} - \tau_{i\theta f} \tag{5}$$

$$\begin{cases} \tau_{i+1,i} = k_{v\theta i}\theta_{i+1,i} \\ \tau_{i,i-1} = k_{v\theta i-1}\theta_{i,i-1} \\ \tau_{i\theta f} = c_{v\theta i}\omega_i, \end{cases} \tag{6}$$

where I_i is the moment of inertia of CA_i. $\tau_{i+1,i}$ and $\tau_{i,i-1}$ denote the torque exerted by $S_{\theta i}$ and $S_{\theta i-1}$, and $\tau_{i\theta f}$ denotes the resistance torque due to the motion of A_i in the polar angle direction. Substituting (6) into (5), we obtain the angle acceleration of CA_i

$$\dot{\omega}_i = \frac{k_{v\theta i}}{I_i}\theta_{i+1,i} - \frac{k_{v\theta i-1}}{I_i}\theta_{i,i-1} - \frac{c_{v\theta i}}{I_i}\omega_i. \tag{7}$$

Then, we obtain the equivalent acceleration of A_i in the angle direction

$$a_{i\theta} = d_i\dot{\omega}_i = \frac{k_{v\theta i}}{I_i}d_i\theta_{i+1,i} - \frac{k_{v\theta i-1}}{I_i}d_i\theta_{i,i-1} - \frac{c_{v\theta i}}{I_i}d_i\omega_i. \tag{8}$$

To reduce the number of parameters of the controller, we use the new parameters k_{ri}, c_{ri}, $k_{\theta i}$, and $c_{\theta i}$, where

$$k_{ri} = \frac{k_{vri}}{m_i}, c_{ri} = \frac{c_{vri}}{m_i}, k_{\theta i} = \frac{k_{v\theta i}}{I_i}, c_{\theta i} = \frac{c_{v\theta i}}{I_i}. \tag{9}$$

Then, we obtain the liquid sphere-inspired decentralized formation controller (10)-(12) for A_i ($i = 1, 2, \dots, N$)

$$a_{ir} = k_{ri}(r_i - d_i) - c_{ri}\dot{d}_i - d_i\omega_i^2 \tag{10}$$

$$a_{i\theta} = k_{\theta i}d_i\theta_{i+1,i} - k_{\theta i-1}d_i\theta_{i,i-1} - c_{\theta i}d_i\omega_i \tag{11}$$

$$\mathbf{a}_i = \begin{bmatrix} \cos\theta_i & \sin\theta_i \\ -\sin\theta_i & \cos\theta_i \end{bmatrix} \begin{bmatrix} a_{i\theta} \\ a_{ir} \end{bmatrix}, \tag{12}$$

where (10) is the radial controller, (11) is the polar angle controller, and (12) transforms $[a_{i\theta}, a_{ir}]'$ into the local world coordinates.

It is worth noting that the liquid sphere-inspired formation controller is decentralized because the controller for A_i only depends on the states of A_i and its two neighbors A_{i-1} and A_{i+1}. In the controller for A_i, the configuration and control parameters are k_{ri}, c_{ri}, r_i, $k_{\theta i}$, and $c_{\theta i}$. $k_{\theta i-1}$ can be obtained by A_i through communication between A_i and A_{i-1}. Other variables in the formation controller can be calculated according to the states of A_i, A_{i-1}, and A_{i+1}.

Theorem 1. *Considering a multiagent system with N agents, using the liquid sphere-inspired formation controller (10)-(12) with the given parameters $k_{ri} > 0$, $c_{ri} > 0$, $r_i > 0$, $k_{\theta i} > 0$, and $c_{\theta i} > 0$ ($i = 1, 2, \dots, N$), the multiagent system globally converges to a unique equilibrium formation.*

Proof. To illustrate the convergence of the liquid sphere-inspired formation control approach, we can equivalently demonstrate the convergence of each d_i and $\theta_{i+1,i}$ ($i = 1, 2, \dots, N$) using the formation controller (10)-(12). Accordingly, the proof of Theorem 1 is decoupled and divided into two vertical directions, ie, the radius direction and the polar angle direction.

Firstly, we demonstrate the proposition that the polar radius d_i globally converges to the desired equilibrium length r_i using the radial controller (10) with $k_{ri} > 0$ and $c_{ri} > 0$. This means that A_i converges to the surface of a virtual liquid sphere with a radius of r_i.

Actually, for the circular motion, we have

$$F_{ir} + m_i d_i\omega_i^2 = m_i\ddot{d}_i. \tag{13}$$

Combining (13) with (10), we get

$$\ddot{d}_i = k_{ri}(r_i - d_i) - c_{ri}\dot{d}_i. \tag{14}$$

Let $\mathbf{X} = [x_1, x_2]' = [d_i, \dot{d}_i]'$ and $\mathbf{Z} = [z_1, z_2]' = [x_1 - r_i, x_2]'$. The differential equation (14) can be transformed into a state-space equation

$$\dot{\mathbf{Z}} = \mathbf{A}\mathbf{Z}, \mathbf{A} = \begin{bmatrix} 0 & 1 \\ -k_{ri} & -c_{ri} \end{bmatrix}. \tag{15}$$

Let $\dot{\mathbf{Z}} = 0$. We obtain the only equilibrium point $\hat{z}_1 = \hat{z}_2 = 0$, which means $\hat{d}_i = \hat{x}_1 = r_i$ and $\dot{\hat{d}}_i = \hat{x}_2 = 0$.

The characteristic equation of (15) is given by

$$\det(\lambda\mathbf{I} - \mathbf{A}) = \lambda^2 + c_{ri}\lambda + k_{ri} = 0. \tag{16}$$

Hence, the characteristic roots are

$$\lambda = \frac{-c_{ri} \pm \sqrt{c_{ri}^2 - 4k_{ri}}}{2}. \tag{17}$$

For $k_{ri} > 0$ and $c_{ri} > 0$, we always have $real(\lambda) < 0$, which means the system of (15) is asymptotically stable. Consequently, the polar radius d_i globally converges to the desired equilibrium length r_i using the radial controller (10) with $k_{ri} > 0$ and $c_{ri} > 0$.

Then, we demonstrate the proposition that the polar angle clearance $\theta_{i+1,i}$ $(i = 1, 2, \dots, N)$ converges to an equilibrium state using the decentralized controllers (11) with the given parameters $k_{\theta i} > 0$ and $c_{\theta i} > 0$.

In the polar angle direction, the multiagent system under control of (11) is a virtual spring network with $c_{\theta i} > 0$. From a perspective of minimizing the energy, the equilibrium formation satisfies

$$\sum_{i=1}^{N} \hat{\theta}_{i+1,i} = 2\pi, \quad k_{\theta i}\hat{\theta}_{i+1,i} = k_{\theta i-1}\hat{\theta}_{i,i-1}, \quad \hat{\dot{\theta}}_i = 0. \tag{18}$$

From (18), we get the unique equilibrium angle clearance

$$\hat{\theta}_{i+1,i} = \frac{2\pi}{\sum_{j=1}^{N} \frac{k_{\theta i}}{k_{\theta j}}}, (i = 1, 2, \dots, N). \tag{19}$$

Let $\mathbf{X}_\theta = [\theta_{2,1}, \dots, \theta_{N,N-1}, \theta_{1,N}, \dot{\theta}_1, \dots, \dot{\theta}_N]'$. We define a Lyapunov function

$$V(\mathbf{X}_\theta) = \frac{1}{2}\sum_{i=1}^{N} k_{\theta i}\left(\theta_{i+1,i} - \hat{\theta}_{i+1,i}\right)^2 + \frac{1}{2}\sum_{i=1}^{N} \dot{\theta}_i^2, \tag{20}$$

then

$$V(\mathbf{X}_\theta) \geqslant 0, \ (V(\mathbf{X}_\theta) = 0, \text{ if and only if } \mathbf{X}_\theta = \hat{\mathbf{X}}_\theta), \tag{21}$$

and

$$\begin{aligned}
\dot{V}(\mathbf{X}_\theta) &= \sum_{i=1}^{N} k_{\theta i}\dot{\theta}_{i+1,i}\left(\theta_{i+1,i} - \hat{\theta}_{i+1,i}\right) + \sum_{i=1}^{N} \dot{\theta}_i\ddot{\theta}_i \\
&= \sum_{i=1}^{N} k_{\theta i}\dot{\theta}_{i+1,i}\theta_{i+1,i} - \sum_{i=1}^{N} k_{\theta i}\dot{\theta}_{i+1,i}\frac{2\pi}{\sum_{j=1}^{N}\frac{k_{\theta i}}{k_{\theta j}}} + \sum_{i=1}^{N}\dot{\theta}_i\left(k_{\theta i}\theta_{i+1,i} - k_{\theta i-1}\theta_{i,i-1} - c_{\theta i}\dot{\theta}_i\right) \\
&= \sum_{i=1}^{N} k_{\theta i}\left(\dot{\theta}_{i+1} - \dot{\theta}_i\right)\theta_{i+1,i} - \frac{2\pi}{\sum_{j=1}^{N}\frac{1}{k_{\theta j}}}\sum_{i=1}^{N}\dot{\theta}_{i+1,i} + \sum_{i=1}^{N} k_{\theta i}\dot{\theta}_i\theta_{i+1,i} - \sum_{i=1}^{N} k_{\theta i-1}\dot{\theta}_i\theta_{i,i-1} - \sum_{i=1}^{N} c_{\theta i}\dot{\theta}_i^2 \\
&= \sum_{i=1}^{N} k_{\theta i}\dot{\theta}_{i+1}\theta_{i+1,i} - \sum_{i=1}^{N} k_{\theta i}\dot{\theta}_i\theta_{i+1,i} + \sum_{i=1}^{N} k_{\theta i}\dot{\theta}_i\theta_{i+1,i} - \sum_{i=1}^{N} k_{\theta i-1}\dot{\theta}_i\theta_{i,i-1} - \sum_{i=1}^{N} c_{\theta i}\dot{\theta}_i^2 \\
&= -\sum_{i=1}^{N} c_{\theta i}\dot{\theta}_i^2 \\
&\leqslant 0, \ (\dot{V}(\mathbf{X}_\theta) = 0, \text{ if and only if } \dot{\theta}_i = \hat{\dot{\theta}}_i = 0, \text{ for } i = 1, 2, \dots, N).
\end{aligned} \tag{22}$$

$\dot{V}(\mathbf{X}_\theta)$ is negative semidefinite. Accordingly, the subsystem in the polar angle direction is Lyapunov stable at $\hat{\mathbf{X}}_\theta$.

To apply the LaSalle invariance principle to establish the local asymptotic stability, we define the set

$$\mathrm{S} = \{\mathbf{X}_\theta | \dot{V}(\mathbf{X}_\theta) = 0\} = \{\mathbf{X}_\theta | \dot{\theta}_i = 0, \text{ for } i = 1, 2, \dots, N\}. \tag{23}$$

S does not contain any trajectory of the system, except $\mathbf{X}_\theta = \hat{\mathbf{X}}_\theta$. Suppose at some time t, $\dot{\theta}_i = 0$, $(i = 1, 2, \dots, N)$. If $\theta_i \neq \hat{\theta}_i$, then $k_{\theta_i}\theta_{i+1,i} = k_{\theta i-1}\theta_{i,i-1}$ can not be satisfied for all $i = 1, 2, \dots, N$. As a result, $\dot{\theta}_i = 0$ cannot be satisfied for all $i = 1, 2, \dots, N$, the trajectory will not stay in the set S.

According to the LaSalle invariance principle, the subsystem in the polar angle direction is asymptotic stable under the control of (11). □

Using the liquid sphere-inspired approach, the unbalanced spring forces (torques) drive the agents. Then, the elastic potential energy is converted into kinetic energy. Meanwhile, the kinetic energy is consumed by the resistance until the formation converges, and all the agents remain still relative to the formation center. This process is similar to that of liquid forming a sphere.

Remark 1. If the parameters in the radius formation controller (10) satisfy $c_{ri} \geqslant 2\sqrt{k_{ri}}$ and $k_{ri} > 0$, the radius d_i converges to the desired equilibrium radius r_i without any overshoot or oscillation.

Using the radius formation controller (10), the closed radius subsystem (15) is a second-order system. From (17), we know that (14) is a second-order over-, critically, and weakly damped system when $c_{ri} > 2\sqrt{k_{ri}}$, $c_{ri} = 2\sqrt{k_{ri}}$, and $0 < c_{ri} < 2\sqrt{k_{ri}}$, respectively. Accordingly, the step response of the system has no overshoot if $c_{ri} \geqslant 2\sqrt{k_{ri}}$ and $k_{ri} > 0$.

Remark 2. The radial formation controller (10) is equivalent to the feedback linearization method combined with the PD control method.

The feedback linearization approach involves creating a transformation of the nonlinear system into an equivalent linear system through a change of variables and a suitable control input. The radius formation controller (10) involves the nonlinear centripetal acceleration $d_i\omega_i^2$ as a nonlinear feedback; then, the control input is transformed from a_{ir} to $\ddot{d}_i$, and the nonlinear system is transformed into a linear system (14). Meanwhile, the first two components in (10) are equivalent to a PD controller with $e = r_i - d_i$, $\dot{e} = -\dot{d}_i$, $K_P = k_{ri}$, and $K_D = c_{ri}$.

The main advantage of the radius formation controller over the traditional feedback linearization and the PD approach is that it has definite physical meaning, which makes the parameters easy to tune in applications (eg, $c_{ri} \geqslant 2\sqrt{k_{ri}}$ and $k_{ri} > 0$).

Remark 3. The final values of the polar angle clearances of all the agents are only determined by $k_{\theta i}$ ($i = 1, 2, \ldots, N$). The relation between them is given by (19). A circular formation, such as that shown in Figure 2B, is obtained when the parameters satisfy $k_{\theta 1} = k_{\theta 2} = \cdots = k_{\theta N} > 0$, $r_1 = r_2 = \cdots = r_N > 0$, $c_{ri} > 0$, and $c_{\theta i} > 0$ ($i = 1, 2, \ldots, N$).

Remark 4. If the parameters in the polar angle controller (11) satisfy $c_{\theta i} \geqslant 2\sqrt{k_{\theta i} + k_{\theta i-1}}$ and $k_{\theta i}, k_{\theta i-1} > 0$ ($i = 1, 2, \ldots, N$), all polar angle clearances converge to the desired equilibrium values without any oscillation, but the avoidance of overshoots cannot be guaranteed.

As an example, $\theta_{3,2}$ in Figure 5 will first increase before it converges back to the desired value $\frac{\pi}{2}$ for $\dot{\omega}_2(0) < 0$ and $\dot{\omega}_3(0) = 0$. Analogously, $\theta_{4,3}$ will first decrease before it converges back to $\frac{\pi}{2}$ for $\dot{\omega}_4(0) > 0$ and $\dot{\omega}_3(0) = 0$.

Remark 5. In applications, the virtual target works as a virtual leader to govern the entire formation. The states of the virtual leader can be stored in each agent so that communication links between a real leader and all the followers are removed, and the formation failure due to the leader's failure is avoided.

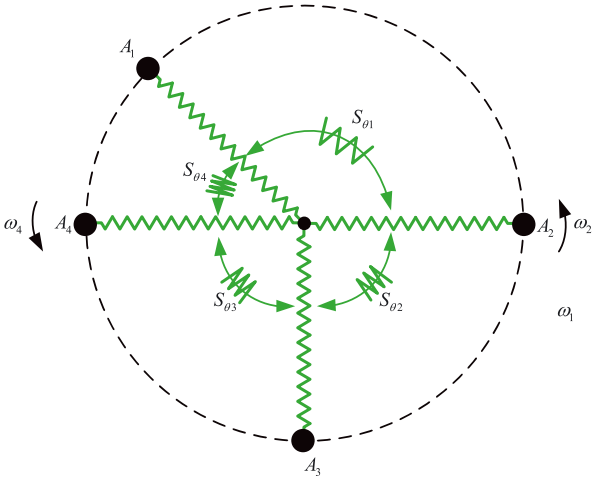

FIGURE 5 An initial state where overshoots cannot be avoided, with parameters $c_{\theta i} \geqslant 2\sqrt{k_{\theta i} + k_{\theta i-1}}$ $k_{\theta i} = k > 0$ and $\omega_i(0) = 0$ for $i = 1, 2, 3, 4$ [Colour figure can be viewed at wileyonlinelibrary.com]

Remark 6. Communication interrupts between agents are not fatal errors for the formation. The formation will maintain or converge to another shape according to the formation states before the communication links break.

Actually, communication interrupts affect the formation only in the polar angle direction. When the communication link between A_i and A_{i+1} breaks, the polar angle θ_i^l and θ_{i+1}^l from the last successful communication can be taken as the real-time states of A_i and A_{i+1} when the two agents receive nothing from each other. If communication interrupts happen after the formation has been constructed, the formation will remain as if the communication is running well. If such failures happen before the formation converge, then θ_i will converge to an equilibrium position between θ_{i-1} and θ_{i+1}^l, and θ_{i+1} will converge to an equilibrium position between θ_i^l and θ_{i+2}.

4 | ARBITRARILY SHAPED FORMATION

Although inspired by the physicomimetics of liquid spheres, the proposed formation control approach is not limited to constructing a circular formation. Actually, different formation shapes can be realized by designing different $k_{\theta i}$ and r_i ($i = 1, 2, \dots, N$). Several examples are given in Figure 6.

Theorem 2. *For a multiagent system with N ($N < \infty$) agents, an arbitrarily shaped formation predefined in Cartesian coordinates can be obtained using the proposed liquid sphere-inspired formation control approach.*

Proof. To obtain a formation predefined in Cartesian coordinates, all we have to know are the virtual formation center C and the corresponding parameters of the controller (10)-(12) for each agent.

A predefined formation is the equilibrium state of the virtual spring network in the liquid sphere-inspired approach. To determine the corresponding parameters of the virtual springs, we first have to find a virtual center C' for the predefined formation such that the corresponding description $(r_i, \hat{\theta}_i)$ of all the agents in the predefined formation satisfies $\hat{\theta}_i > \hat{\theta}_j$ ($i > j$) and $r_i > 0$.

To this end, we use $l_{ij} = Span\{\mathbf{p}_i, \mathbf{p}_j\}$ to denote a point set including all the points on the straight line through the ith and jth agents in the predefined formation. S means the $O - XY$ space. Then, $L = \bigcup l_{ij}$ is a union of C_N^2 lines in the $O - XY$ plane. For $C_N^2 = \frac{N(N-1)}{2} < \infty$, $L \subset S$, which means $S - L \neq \Phi$. Then, any point in $\mathbf{int}(S - L)$ can be selected as the virtual center C' because any ray from a point in $\mathbf{int}(S - L)$ goes through no more than one agent in the predefined formation. Therefore, in the polar coordinates system centered by $C' \in \mathbf{int}(S - L)$, we always have $(r_i, \hat{\theta}_i)$ with $\hat{\theta}_i \neq \hat{\theta}_j$ ($i \neq j$) and $r_i > 0$. By relabeling the agents, we obtain $\hat{\theta}_i > \hat{\theta}_j$, for $i > j$.

Accordingly, we obtain $\hat{\theta}_{i+1,i} = \hat{\theta}_{i+1} - \hat{\theta}_i$ ($i = 1, 2, \dots, N-1$) and $\hat{\theta}_{1,N} = \hat{\theta}_1 - \hat{\theta}_N + 2\pi$.

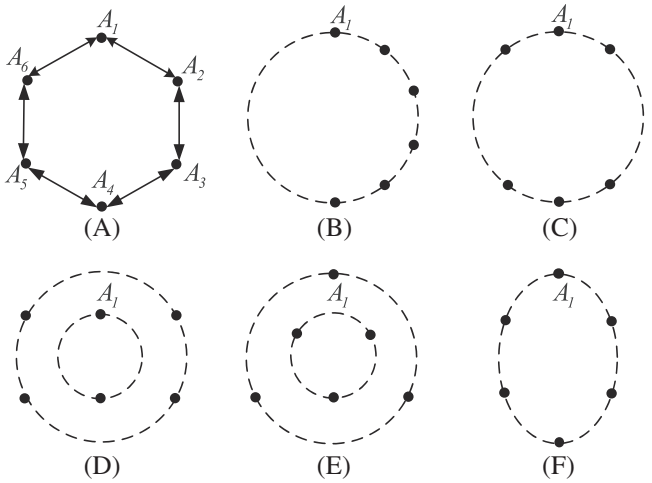

FIGURE 6 Some examples of different shapes that can be obtained using different $k_{\theta i}$ (eg, B and C) or different r_i (eg, D, E, and F). Configurations: A, $k_{\theta 1} = \cdots = k_{\theta 6}$ and $r_1 = \cdots = r_6$; B, $k_{\theta 1} = \cdots = k_{\theta 5} = 5k_{\theta 6}$ and $r_1 = \cdots = r_6$; C, $k_{\theta 1} = k_{\theta 3} = k_{\theta 4} = k_{\theta 6} = 4k_{\theta 2} = 4k_{\theta 5}$ and $r_1 = \cdots = r_6$; D, $k_{\theta 1} = \cdots = k_{\theta 6}$ and $2r_1 = 2r_4 = r_2 = r_3 = r_5 = r_6$; E, $k_{\theta 1} = \cdots = k_{\theta 6}$ and $r_1 = 2r_2 = r_3 = 2r_4 = r_5 = 2r_6$; F, $k_{\theta 1} = \cdots = k_{\theta 6}$ and $r_i = \sqrt{a^2\cos^2(\frac{(i-1)\pi}{3}) + b^2\sin^2(\frac{(i-1)\pi}{3})}$, where a and b are the semiaxes of the ellipsoid

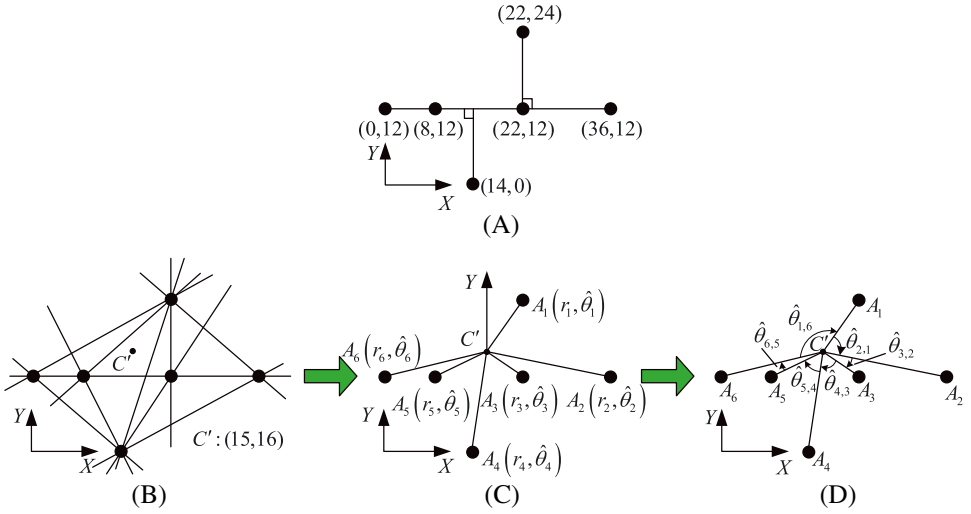

FIGURE 7 An example of an arbitrarily shaped formation. A, The desired formation shape described in the Cartesian coordinates; B-D, The procedure to design the formation controller [Colour figure can be viewed at wileyonlinelibrary.com]

Letting $k_{\theta 1} = k > 0$ and making use of the relation in (18), we get

$$k_{\theta i} = \frac{\hat{\theta}_{2,1}}{\hat{\theta}_{i+1,i}} k, \quad \left(i = 1, 2, \ldots, N \text{ and } \hat{\theta}_{N+1,N} = \hat{\theta}_{1,N}\right). \tag{24}$$

Other parameters, including k_{ri}, c_{ri}, and $c_{\theta i}$, can be determined according to Remarks 1 and 2.

Then, we have to find a virtual center C according to the initial states of the multiagent system. The procedure is similar to the determination of C'. By labeling all the agents in the multiagent system, we obtain $\theta_i > \theta_j$, for $i > j$. Then, the information of C and the parameters determined earlier can be applied in the liquid sphere-inspired controller for each agent to obtain the predefined formation. □

An example is introduced to demonstrate the procedure to design the decentralized controller for an arbitrarily shaped formation.

Example 1. The procedure to obtain the formation in Figure 7A is given by the following.

- **Step 1**: Connect every two agents using a straight line and obtain C_N^2 lines l_{ij} and $L = \bigcup l_{ij}$. Here, $N = 6$ and $C_N^2 = 15$.
- **Step 2**: Arbitrarily select a point $C' \in \mathbf{int}(S - L)$, and define C' as the virtual center in the predefined formation. Here, we define $C' = (15, 16) \in \mathbf{int}\,(S - L)$.
- **Step 3**: Calculate the desired polar radius and angle of each agent in the formation coordinates $C' - XY$. Relabel the agents so that $\hat{\theta}_i > \hat{\theta}_j$, for $i > j$. Here, we get

$$\begin{aligned} \left[\hat{\theta}_1, \hat{\theta}_2, \hat{\theta}_3, \hat{\theta}_4, \hat{\theta}_5, \hat{\theta}_6\right]' &= [0.7188, 1.7590, 2.0899, 3.2040, 4.1932, 4.4518]' \\ [r_1, r_2, r_3, r_4, r_5, r_6]' &= [10.6301, 21.3776, 8.0623, 16.0312, 8.0623, 15.5242]'. \end{aligned} \tag{25}$$

- **Step 4**: Calculate the polar angle clearances $\hat{\theta}_{i+1,i} = \hat{\theta}_{i+1} - \hat{\theta}_i$ $(i = 1, 2, \ldots, 5)$ and $\hat{\theta}_{1,N} = \hat{\theta}_1 - \hat{\theta}_N + 2\pi$. Here, we get

$$\left[\hat{\theta}_{2,1}, \hat{\theta}_{3,2}, \hat{\theta}_{4,3}, \hat{\theta}_{5,4}, \hat{\theta}_{6,5}, \hat{\theta}_{1,6}\right]' = [1.0402, 0.3309, 1.1141, 0.9892, 0.2586, 2.5502]'. \tag{26}$$

- **Step 5**: Letting $k_{\theta 1} = 1 > 0$ and calculating $k_{\theta i}$ according to (24), we get

$$[k_{\theta 1}, k_{\theta 2}, k_{\theta 3}, k_{\theta 4}, k_{\theta 5}, k_{\theta 6}]' = [1, 3.1433, 0.9337, 1.0515, 4.0233, 0.4079]'. \tag{27}$$

- **Step 6**: Letting $k_{ri} = 1$ and calculating c_{ri} and $c_{\theta i}$ according to $c_{ri} = 2\sqrt{k_{ri}}$ and $c_{\theta i} = 2\sqrt{k_{\theta i} + k_{\theta i-1}}$ $(i = 1, 2, \ldots, 6)$, we get

$$\begin{aligned} [c_{r1}, c_{r2}, c_{r3}, c_{r4}, c_{r5}, c_{r6}]' &= [2, 2, 2, 2, 2, 2]' \\ [c_{\theta 1}, c_{\theta 2}, c_{\theta 3}, c_{\theta 4}, c_{\theta 5}, c_{\theta 6}]' &= [2.3731, 4.0710, 4.0383, 2.8179, 4.5055, 4.2101]'. \end{aligned} \tag{28}$$

- **Step 7**: Determine a virtual formation center C according to the initial states of the agents and apply the parameters determined earlier in the proposed controller for each agent.

With the procedure, the multiagent system converges to the formation predefined in Figure 7A. It is worth noting that this is not the only solution to realize the desired formation because different selections of C' produce different solutions.

5 | OTHER EXTENSIONS

In this section, we further discuss various good properties and abilities of the proposed liquid sphere-inspired physicomimetics formation control approach, including scalability, formation change, and obstacle avoidance.

5.1 | Scalability

In our work, the structure of the proposed liquid sphere-inspired formation control approach is decentralized, which allows the approach to have better scalability for dynamically adding or removing agents than the centralized approaches. Moreover, an extra agent can be added to a formation using the proposed approach like mixing a drop into a sphere of liquid.

Considering that all the agents have the same control parameters, we obtain a circular formation. To include an extra agent with the same parameters in the circular formation, the work required is to partially change the communication topology around the extra agent without damaging the entire former formation. There is no need to modify any control parameters or the configuration of any agent in the former formation.

We assume that the extra agent can detect the closest two agents and take them as its two neighbors. Then, the work required to add the new agent to the formation is to cut off the communication connection between its two neighbors and simultaneously build up two new connections between the new agent to its two neighbors. Finally, the unbalanced virtual (angle) springs force the agent to converge to the circular formation. Figure 8A shows the schematic diagram of the procedure of dynamically adding an agent into a formation of five agents. Analogously, to remove an agent from a formation, the required work is to cut off the communication connections between the agent and its two neighbors and simultaneously build up a new connection between the two neighbors. Figure 8B shows the schematic diagram of the procedure of dynamically removing an agent from a formation of five agents.

5.2 | Switching between formations

As mentioned in Section 4, the liquid sphere-inspired formation control approach is not limited to constructing a circular formation. Actually, we can dynamically switch a formation shape from one to another by dynamically changing the parameters of the virtual (angle) springs. For instance, the formation shape can be transformed from Figure 6A to Figure 6B by changing one parameter $k_{\theta 6}$ into $0.2k_{\theta 5}$. Similarly, we can obtain a transformation from Figure 6A to Figure 6E by halving the desired radii r_2, r_4, and r_6.

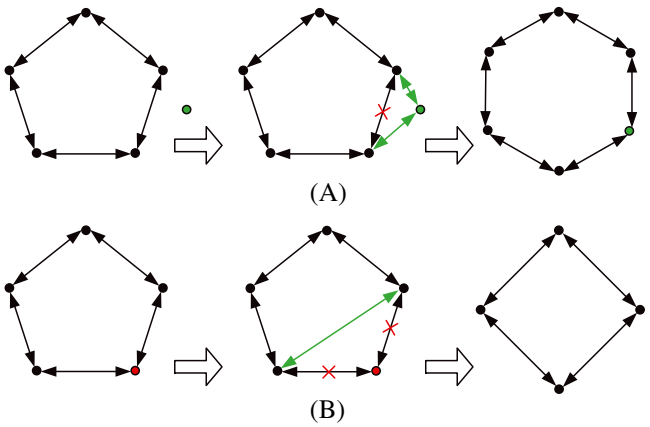

FIGURE 8 The schematic diagram of the procedures of (A) dynamically adding an agent to a formation and (B) removing an agent from a formation [Colour figure can be viewed at wileyonlinelibrary.com]

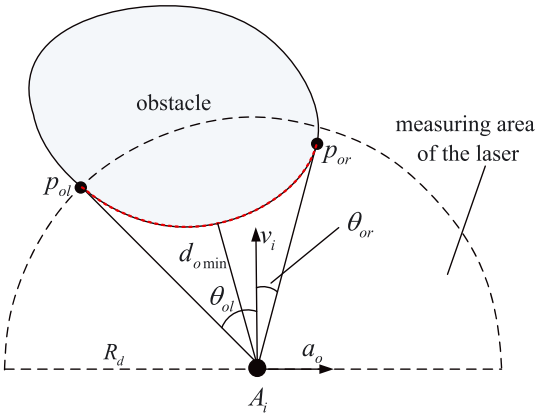

FIGURE 9 Diagram of avoidance of an obstacle using the liquid sphere-inspired physicomimetics approach [Colour figure can be viewed at wileyonlinelibrary.com]

Using the liquid sphere-inspired approach, interagent collisions are resisted by the virtual forces (or torques). This is because collisions between adjacent agents are brought about by motions that produce an imbalance along the formation circle, whereas, in the liquid sphere-inspired approach, any motion that produces an imbalance between adjacent agents is resisted by the resistance and the unbalanced virtual angle springs. In the transformation, the agents are expected to converge from a former equilibrium state to a new one. Collisions between adjacent agents can be prevented if the drag coefficients are large enough ($c_{ri} \geqslant 2\sqrt{k_{ri}}$ and $c_{\theta i} \geqslant 2\sqrt{k_{\theta i} + k_{\theta i-1}}$, $(i = 1, 2, \ldots, N)$) to prevent overshoots or oscillations.

5.3 | Obstacle avoidance

It is important for a multiagent system to have the ability to dynamically avoid obstacles. When static obstacles pop up during the formation, the agents are required to move out of their way to steer around them and also avoid collisions between each other. After that, the agents should go back to their proper places. To achieve these goals, a repulsive force from the obstacle is designed. Then, the formation can avoid obstacles like fluid flowing over obstacles.

The following assumption is made in this section.

Assumption 2. Every agent is equipped with a laser to sense the local obstacles. Accordingly, an agent acquires a point set $P_o = \{(d_o, \theta_o) | d_o \leq R_d, -\frac{\pi}{2} < \theta_o < \frac{\pi}{2}\}$ on the surface of the obstacle in the local polar coordinates when an obstacle is detected, where the positive direction of θ_o is clockwise and R_d is the detection radius of the laser, as shown in Figure 9.

Based on Assumption 2, when an obstacle is detected by an agent, the leftmost point $p_{ol} = (d_{ol}, \theta_{ol})$ and the rightmost point $p_{or} = (d_{or}, \theta_{or})$ in the view of the local agent can be determined form P_o. d_{omin} denotes the closed distance between the agent and the obstacle detected by the laser.

We design an extra virtual repulsive force that repels the agent in the lateral direction. Without any prior knowledge of the world, it is reasonable for the agent to avoid the obstacle along the side with the smaller angle of view. Accordingly, the obstacle repels the agent to the right when $|\theta_{or}| \leq |\theta_{ol}|$ and to the left when $|\theta_{or}| > |\theta_{ol}|$.

The extra acceleration a_o due to the obstacle can be calculated by

$$a_o = (1 + \alpha v_i) k_o l_o, \tag{29}$$

where $\alpha \in [0, 1]$, $k_o = \frac{r_i * k_{ri}}{r_c}$, and r_c is the allowed minimum clearance between the agent and the obstacle. l_o is calculated by

$$l_o = \begin{cases} d_{ol}\sin(\theta_{ol}) - r_c & -\theta_{or} \leqslant \theta_{ol} < 0 \\ d_{or}\sin(\theta_{or}) + r_c & 0 \leqslant \theta_{or} < -\theta_{ol} \\ d_{omin} - 2r_c & \theta_{ol} \geqslant \max\{0, -\theta_{or}\}, d_{omin} < 2r_c \\ 2r_c - d_{omin} & \theta_{or} < \min\{0, -\theta_{ol}\}, d_{omin} < 2r_c \\ 0, & \text{else.} \end{cases} \tag{30}$$

Then, the decentralized formation controller (12) can be modified using the extra acceleration a_o by

$$\mathbf{a}_i = \begin{bmatrix} \cos\theta_i & \sin\theta_i \\ -\sin\theta_i & \cos\theta_i \end{bmatrix} \begin{bmatrix} a_{i\theta} \\ a_{ir} \end{bmatrix} + \begin{bmatrix} a_o\cos(\psi_i) \\ -a_o\sin(\psi_i) \end{bmatrix}, \tag{31}$$

where ψ_i is the heading angle of A_i.

When the multiagent system avoids obstacles, collisions between the agents are resisted by unbalanced virtual angle springs, which is similar to the surface tension on a liquid sphere. It is worthwhile to note that this is not the only way to modify the approach to avoid obstacles, as one can design other types of repulsive forces to do so. This simple modification is just used to illustrate the potential ability of the novel physicomimetics approach to avoid obstacles.

6 | SIMULATION RESULTS

This section presents simulation results to illustrate the effectiveness of the proposed approach. An SPF-based approach in the work of Olfati-Saber and Murray[16] is selected as the comparative approach. The aforementioned work[16] used a metric formation graph to describe a formation. An MGF is a triplet $\mathbf{G} = (\mathbf{V}_e, \mathbf{C}, \mathbf{D})$, where $\mathbf{V}_e$ is the expanding set of the vertices, $\mathbf{C}$ is the connectivity matrix, and $\mathbf{D}$ is the distance matrix. To realize the desired formation, they made use of natural potential functions obtained from structural constraints of a desired formation. In the following, the convergence, scalability, and flexibility of the proposed approach are evaluated by numerical simulations.

6.1 | Convergence to a circular formation

In this scenario, the 6 agents (A_1 through A_6) are located at (5, 5), (15, −7), (7, −15), (−10, −25), (−5, −10), and (−10, 0), respectively, and are initially still. The proposed liquid sphere-inspired approach (10)-(12) is applied to construct a circular formation with a radius of 10 m, and the parameters of the decentralized formation controllers are given by

$$k_{ri} = k_{\theta i} = 1,\ c_{ri} = 2,\ c_{\theta i} = 2\sqrt{2},\ r_i = 10 (i = 1, 2, \ldots, 6). \tag{32}$$

To obtain the same formation using the SPF-based approach in the work of Olfati-Saber and Murray,[16] the information graph and formation shape should be given as shown in Figure 10. Then, the corresponding connectivity matrix $\mathbf{C}$ and distance matrix $\mathbf{D}$ are given in (33). The distributed controller from the aforementioned work[16] for each agent is rewritten via (34). Considering the same initial states and using the recommended parameters in the work of Olfati-Saber and Murray,[16] $\bar{a} = 10$ and $\lambda_1 = \lambda_2 = 0.5$, and then the simulation results of the SPF-based approach are shown by the dashed line in Figure 11

$$\mathbf{C} = \begin{bmatrix} A_2 & A_4 & A_6 & A_\infty & A_\infty \\ A_1 & A_3 & A_3 & A_5 & A_6 \\ A_2 & A_4 & A_6 & A_\infty & A_\infty \\ A_1 & A_2 & A_3 & A_5 & A_6 \\ A_2 & A_4 & A_6 & A_\infty & A_\infty \\ A_1 & A_2 & A_3 & A_4 & A_5 \end{bmatrix},\ \mathbf{D} = \begin{bmatrix} 10 & 20 & 10 & \infty & \infty \\ 10 & 10 & 10\sqrt{3} & 20 & 10\sqrt{3} \\ 10 & 10 & 20 & \infty & \infty \\ 20 & 10\sqrt{3} & 10 & 10 & 10\sqrt{3} \\ 20 & 10 & 10 & \infty & \infty \\ 10 & 10\sqrt{3} & 20 & 10\sqrt{3} & 10 \end{bmatrix} \tag{33}$$

$$\mathbf{a}_i = \frac{\bar{a}}{|J_i|} \sum_{j \in J_i} \lambda_1 \sigma_1(\|\mathbf{x}_i - \mathbf{x}_j\| - d_{ij})\mathbf{u}_{ij} - \bar{a}\lambda_2\sigma_2(\mathbf{v}_i). \tag{34}$$

To make the results more comparable, the center of the final formation using the SPF-based approach is determined as the virtual center of the liquid sphere-inspired approach. Then, the trajectories using the liquid sphere-inspired approach are shown by the solid line in Figure 11. The results show that a circular formation can be obtained using either of the two approaches. In the SPF-based approach, only distance configurations between agents are considered, and thus more connections (no less than $2N - 3$) are required to guarantee a unique desired formation. In comparison to the SPF-based approach, the liquid sphere-inspired approach requires fewer communication links (N) when the number of agents $N > 3$.

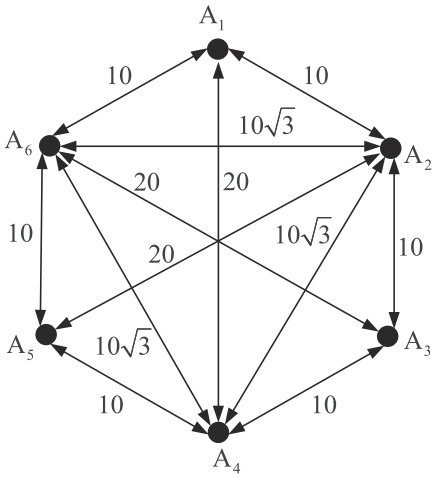

FIGURE 10 A metric formation graph of an orthohexagonal formation with six agents

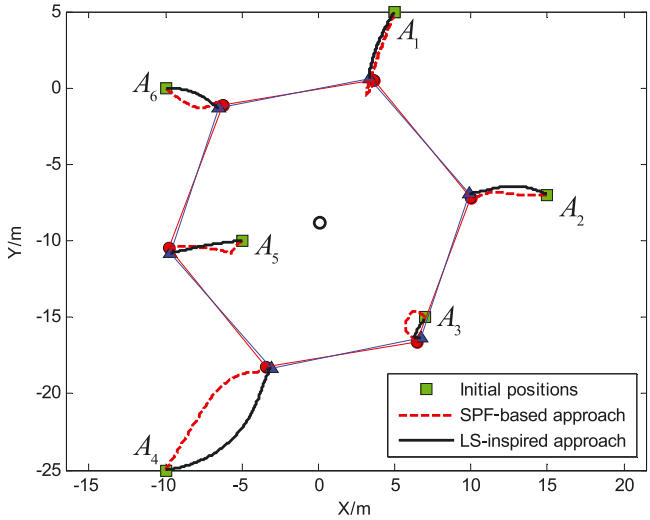

FIGURE 11 Trajectories of the agents in the simulation of a six-agent formation. SPF, structural potential function [Colour figure can be viewed at wileyonlinelibrary.com]

Figure 12 gives the angle clearances and radii of the agents throughout the simulation using the liquid sphere-inspired approach. It shows that the polar radii of all the agents converge to 10 m without any overshoot. The angle clearances converge to the equilibrium value $\frac{\pi}{3}$ without oscillations, but slight overshoots exist for $\theta_{3,2}$, $\theta_{4,3}$, and $\theta_{1,6}$.

6.2 | Arbitrarily shaped formation

In this scenario, we give the simulation results of Example 1. The agents, ie, A_1 through A_6, are initially still at $(22, 24)$, $(40, 25)$, $(30, 10)$, $(15, 10)$, $(10, 0)$, and $(5, 20)$, respectively. The liquid sphere-inspired approach and the parameters designed in Example 1 are applied. The point (15,16) is selected as the virtual center. The simulation results using the liquid sphere-inspired approach and the SPF-based approach are shown in Figure 13. The simulation results show that the agents converge to the predefined formation in Figure 7A using both of the two approaches.

6.3 | Dynamically adding an agent to a circular formation

In this scenario, we dynamically add an extra agent to a five-agent formation. Initially, five agents are uniformly distributed along a circle with a radius of 10 m, and these agents, ie, A_1 through A_5, are located at $(0, 10)$, $(10\sin(\frac{2\pi}{5}), 10\cos(\frac{2\pi}{5}))$, $(10\sin(\frac{4\pi}{5}), 10\cos(\frac{4\pi}{5}))$, $(10\sin(\frac{6\pi}{5}), 10\cos(\frac{6\pi}{5}))$, and $(10\sin(\frac{8\pi}{5}), 10\cos(\frac{8\pi}{5}))$, respectively. The initial position of the extra agent A_a is $(20, 5)$.

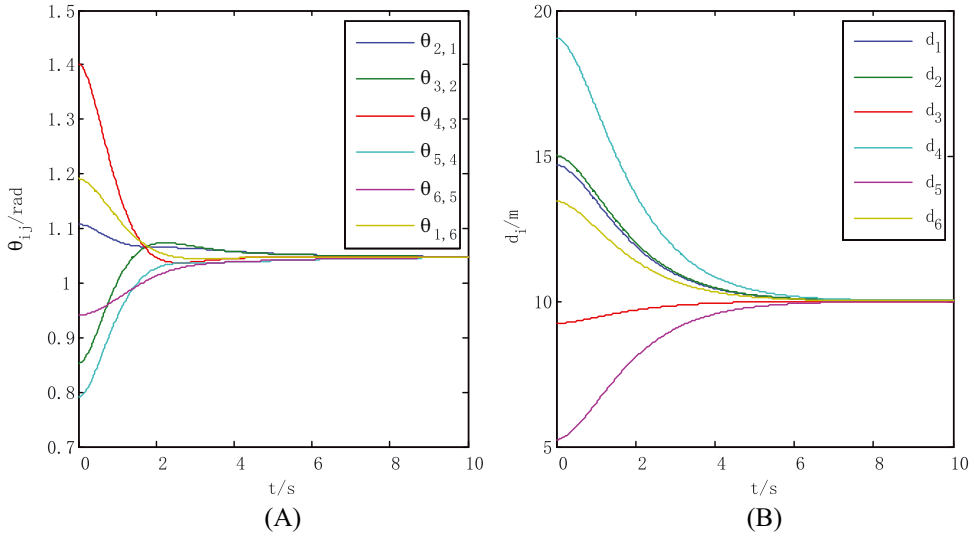

FIGURE 12 Polar angle clearances (A) and polar radii (B) of the agents using the liquid sphere-inspired approach [Colour figure can be viewed at wileyonlinelibrary.com]

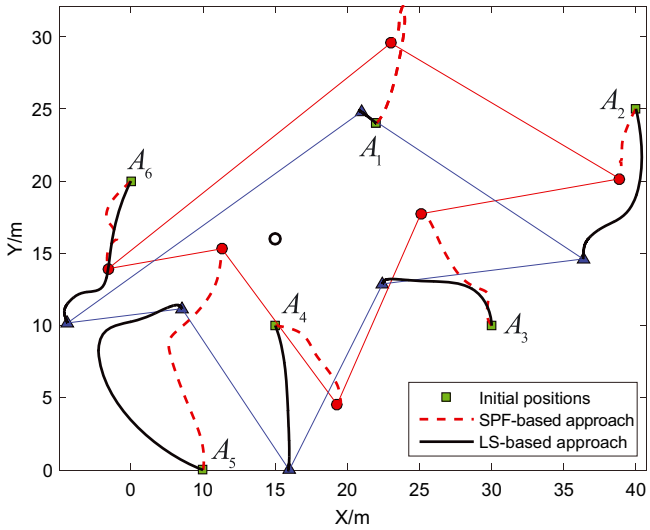

FIGURE 13 Trajectories of all the agents throughout the arbitrarily shaped formation simulation. SPF, structural potential function [Colour figure can be viewed at wileyonlinelibrary.com]

The virtual center is $(0, 0)$. The initial parameters of the liquid sphere-inspired controllers for the five agents are

$$k_{ri} = k_{\theta i} = 1,\ c_{ri} = 2,\ c_{\theta i} = 2\sqrt{2},\ r_i = 10 (i = 1, 2, \ \dots\ , 5). \tag{35}$$

To add A_a to the formation, we have to cut off the communication link between A_2 and A_3 and simultaneously create two new links connecting A_a with A_2 and A_3. A_a uses the same parameters as the other agents.

Figure 14A shows the process of adding an agent A_a to a circular formation. Although the new agent makes the formation enter a state of disequilibrium, the unbalanced surface tension and the molecular force modeled by the virtual (angle) springs force the formation to regain equilibrium asymptotically. The result in Figure 14A is similar to the process of mixing a drop of liquid into a liquid sphere. Thus, it is flexible to the dynamic addition of an extra agent into the formation using the proposed liquid sphere-inspired approach. The work required is to partially reconfigure the local communication.

Although the SPF-based approach in the work of Olfati-Saber and Murray[16] can also be used to add an agent to a formation, one has to redesign the connectivity matrix **C** and the distance matrix **D** according to the desired formation. Then, all the distributed controllers for the formation are changed according to **C** and **D**. Considering the same initial

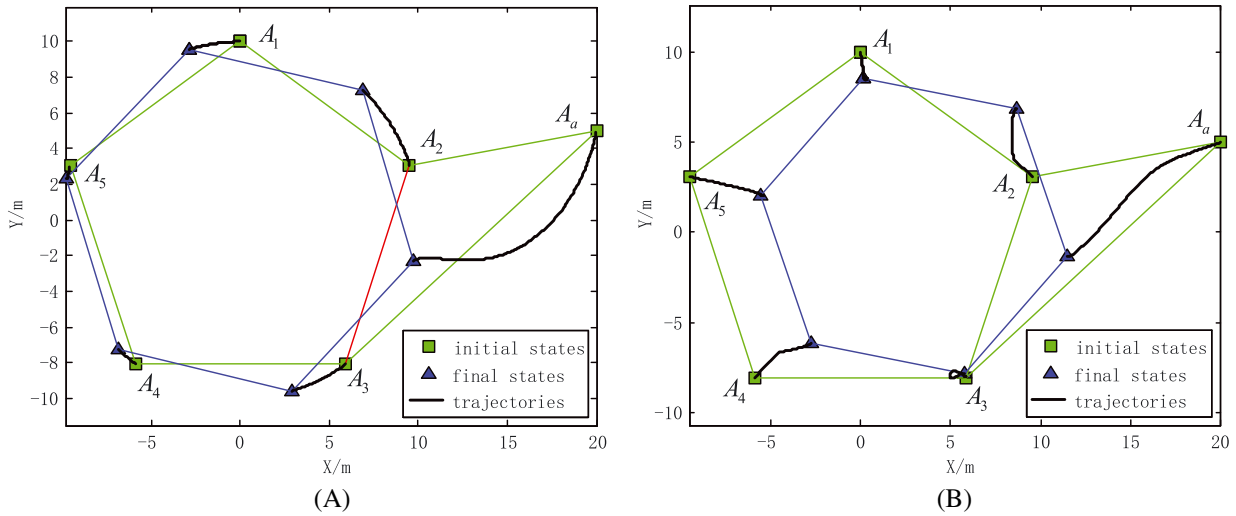

FIGURE 14 Simulation results for adding an extra agent to a five-agent formation. A, Using the liquid sphere-inspired approach; B, using the SPF-based approach. SPF, structural potential function [Colour figure can be viewed at wileyonlinelibrary.com]

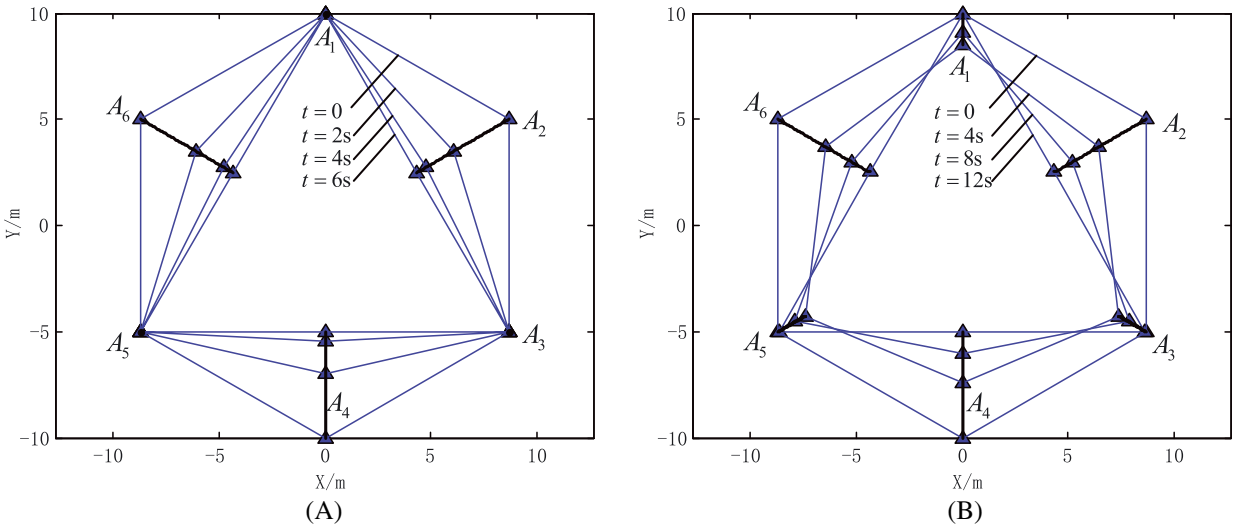

FIGURE 15 Simulation results of changing a circular formation into a triangular formation. A, Using the liquid sphere-inspired approach; B, using the SPF-based approach. SPF, structural potential function [Colour figure can be viewed at wileyonlinelibrary.com]

states and using the recommended parameters in the aforementioned work,[16] $\bar{a} = 10$ and $\lambda_1 = \lambda_2 = 0.5$; the simulation results of the SPF-based approach are shown in Figure 14B.

6.4 | Switching between formations

In this scenario, we give the simulation result of switching a six-agent team from a circular formation to a triangular formation. Initially, six agents are uniformly distributed along a circle with a radius of 10 m, on which the agents, ie, A_1 through A_6, are located at $(0, 10)(5\sqrt{3}, 5)$, $(5\sqrt{3}, -5)$, $(0, -10)$, $(-5\sqrt{3}, -5)$, and $(-5\sqrt{3}, 5)$, respectively. The virtual center is $(0, 0)$. The initial parameters of the liquid sphere-inspired controllers for the six agents are given in (32).

To obtain a triangular formation using the liquid sphere-inspired approach, we only have to adjust the desired polar radii of A_2, A_4, and A_6 to be 5 m, without changing any other parameters in (32). Then, the new configuration makes the formation enter a state of disequilibrium, and the unbalanced forces of the virtual springs S_{r2}, S_{r4}, and S_{r6} force the formation to regain equilibrium. Figure 15A shows the result of switching a circular formation to a triangular formation. The new formation regains equilibrium in 6 *s*. There are no overshoots of d_2, d_4, and d_6. In addition, A_1, A_3, and A_5 remain still throughout the simulation.

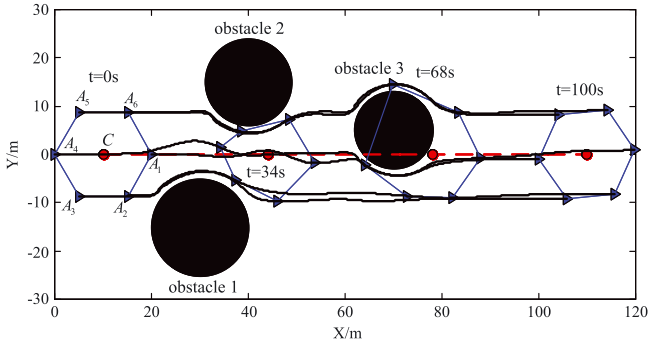

FIGURE 16 Simulation results of obstacle avoidance using a six-agent circular formation [Colour figure can be viewed at wileyonlinelibrary.com]

To obtain the same transformation using the SPF-based approach, a new distance matrix is required as follows

$$\mathbf{D}_{\text{new}} = \begin{bmatrix} 5\sqrt{3} & 15 & 5\sqrt{3} & \infty & \infty \\ 5\sqrt{3} & 5\sqrt{3} & 5\sqrt{3} & 15 & 5\sqrt{3} \\ 5\sqrt{3} & 5\sqrt{3} & 15 & \infty & \infty \\ 15 & 5\sqrt{3} & 5\sqrt{3} & 5\sqrt{3} & 5\sqrt{3} \\ 15 & 5\sqrt{3} & 5\sqrt{3} & \infty & \infty \\ 5\sqrt{3} & 5\sqrt{3} & 15 & 5\sqrt{3} & 5\sqrt{3} \end{bmatrix}. \tag{36}$$

Then, all the SPF-based distributed controllers for the six agents have to be reconfigured because all the rows of the distance matrix are changed (compare $\mathbf{D}_{\text{new}}$ with $\mathbf{D}$). Considering the same initial states and using the recommended parameters in the work of Olfati-Saber and Murray,[16] $\bar{a} = 10$ and $\lambda_1 = \lambda_2 = 0.5$; the simulation results of the SPF-based approach are shown in Figure 15B. The new formation converges to a triangular formation in 12 s. A_2, A_4, and A_6 converge to the desired positions without overshoots, but A_1, A_3, and A_5 are firstly pulled into the circle before converging back to the desired positions.

6.5 | Avoiding obstacles

In this scenario, a six-agent formation is simulated to demonstrate obstacle avoidance. The modified controller (31) is applied. Initially, an equilibrium formation of six agents is moving with the virtual center C along the $X-$ axis at a speed of $v_c = 1$ m/s, and the parameters are given by

$$\begin{aligned} &k_{ri} = k_{\theta i} = 0.2,\ c_{ri} = 2\sqrt{0.2}, c_{\theta i} = 2\sqrt{0.4},\ r_i = 10 (i = 1, 2, \ldots, 6) \\ &R_d = 3, r_c = 1,\ \alpha = 0.5. \end{aligned} \tag{37}$$

Three circular obstacles are located at $(30, -15)$, $(40, 15)$, and $(70, 5)$. The radii of the three obstacles are 10 m, 9 m, and 8 m, respectively. Figure 16 shows the simulation results using the liquid sphere-inspired approach. It shows that the formation is flexible enough to avoid the obstacles. When obstacle 1 is detected by A_2 and A_3, the extra repulsive forces repel A_2 and A_3 to the left to maneuver around obstacle 1. Analogously, obstacle 2 repels A_5 and A_6 to the right to maneuver around it. Accordingly, the six-agent formation squeezes through the narrow passage between obstacles 1 and 2. When obstacle 3 is detected, A_1 and A_4 are repelled to the right and A_5 and A_6 are repelled to the left to maneuver around it. Throughout the simulation, every agent reacts to its neighbors' motion to avoid a collision between them. As a result, a formation can avoid obstacles using the liquid sphere-inspired approach, like a liquid flowing over obstacles or squeezing through narrow passages.

7 | CONCLUSION

In this paper, a liquid sphere-inspired physicomimetics approach has been proposed for multiagent formation control. The formation was formulated as a liquid sphere by modeling the intermolecular force and the surface tension using

virtual forces of imaginary springs. It gave the proposed approach various properties of a liquid sphere. Using the proposed approach, an extra agent could be added to a formation like mixing a drop of liquid into a liquid sphere, and a formation could avoid obstacles like a liquid flowing over obstacles or squeezing through narrow passages. The liquid sphere-inspired approach was decentralized, and each agent only communicated with its two neighbors. The liquid sphere-inspired approach was founded on solid physical theory and was computationally simple due to the use of artificial physics. Moreover, the physical meanings of the parameters were definite, which makes it easy to tune in applications. Simulation results have demonstrated the effectiveness of the proposed approach.

We believe that the liquid sphere-inspired physicomimetics approach is not only applicable for simple multiagent systems, and we will extend the approach for complicated agents, such as robots, aircrafts, and UAVs. Further testing will be conducted on the multi-UAV system developed in the work of Wang et al.[28] Besides, future work will consider Cartesian distance between the agents in the definition of neighbors. Moreover, the robustness of the approach to communication delay and loss of information will be investigated in the future.

ACKNOWLEDGEMENTS

The authors appreciate the constructive comments and suggestions of the reviewers. This work was supported by the Research Project of the National University of Defense Technology (no. JC-13-03-02) and the National Natural Science Foundation of China (grant 61403406).

ORCID


Xun Wang http://orcid.org/0000-0002-4334-2145

REFERENCES

1. Anderson BD, Yu C, Hendrickx JM. Rigid graph control architectures for autonomous formations. *IEEE Control Syst Mag*. 2008;28(6):48-63.
2. Wang X, Qin J, Yu C. ISS method for coordination control of nonlinear dynamical agents under directed topology. *IEEE Trans Cybern*. 2014;44(10):1832-1845.
3. Wang X, Yu C, Lin Z. A dual quaternion solution to attitude and position control for rigid-body coordination. *IEEE Trans Robot*. 2012;28(5):1162-1170.
4. Milln P, Orihuela L, Jurado I, Rubio FR. Formation control of autonomous underwater vehicles subject to communication delays. *IEEE Trans Control Syst Technol*. 2014;22(2):770-777.
5. Ahn H-S. Leader–follower type relative position keeping in satellite formation flying via robust exponential stabilization. *Int J Robust Nonlinear Control*. 2012;22(18):2084-2099.
6. Zhao Y, Duan Z, Wen G, Chen G. Distributed finite-time tracking of multiple non-identical second-order nonlinear systems with settling time estimation. *Automatica*. 2016;64:86-93.
7. Gustavi T, Hu X. Observer-based leader-following formation control using onboard sensor information. *IEEE Trans Robot*. 2008;24(6):1457-1462.
8. Mariottini GL, Morbidi F, Prattichizzo D, et al. Vision-based localization for leader-follower formation control. *IEEE Trans Robot*. 2009;25(6):1431-1438.
9. Chen X, Yan P, Serrani A. On input-to-state stability-based design for leader/follower formation control with measurement delays. *Int J Robust Nonlinear Control*. 2013;23(13):1433-1455.
10. Ren W, Beard R. Decentralized scheme for spacecraft formation flying via the virtual structure approach. *J Guid Control Dyn*. 2004;27(1):73-82.
11. Sadowska A, Broek T, Huijberts H, van de Wouw N, Kostić D, Nijmeijer H. A virtual structure approach to formation control of unicycle mobile robots using mutual coupling. *Int J Control*. 2011;84(11):1886-1902.
12. Watanabe Y, Amiez A, Chavent P. Fully-autonomous coordinated flight of multiple UAVs using decentralized virtual leader approach. Paper presented at: 2013 IEEE/RSJ International Conference on Intelligent Robots and Systems; 2013; Tokyo, Japan.
13. Giulietti F, Pollini L, Innocenti M. Formation flight control - a behavioral approach. Paper presented at: AIAA Guidance, Navigation, and Control Conference and Exhibit; 2001; Montreal, Canada.
14. Lawton JRT, Beard RW, Young BJ. A decentralized approach to formation maneuvers. *IEEE Trans Robot Autom*. 2003;19(6):933-941.
15. Fax JA, Murray RM. Graph Laplacians and stabilization of vehicle formations. *IFAC Proc Vol*. 2001;35(1):55-60.
16. Olfati-Saber R, Murray RM. Distributed cooperative control of multiple vehicle formations using structural potential functions. *IFAC Proc Vol*. 2001;35(1):495-500.
17. Gazi V. Swarm aggregations using artificial potentials and sliding-mode control. *IEEE Trans Robot*. 2005;21(6):1208-1214.

18. Mabrouk MH, McInnes CR. Solving the potential field local minimum problem using internal agent states. *Robot Auton Syst*. 2008;56(12):1050-1060.
19. Liu Y, Zhao Y, Chen G. Finite-time formation tracking control for multiple vehicles: a motion planning approach. *Int J Robust Nonlinear Control*. 2016;26(14):3130-3149.
20. Oh K-K, Park M-C, Ahn H-S. A survey of multi-agent formation control. *Automatica*. 2015;53:424-440.
21. Cao Y, Yu W, Ren W, Chen G. An overview of recent progress in the study of distributed multi-agent coordination. *IEEE Trans Ind Inform*. 2013;9(1):427-438.
22. Wang X, Zeng Z, Cong Y. Multi-agent distributed coordination control: developments and directions via graph viewpoint. *Neurocomputing*. 2016;199:204-218.
23. Spears WM, Spears DF, Hamann JC, Heil R. Distributed, physics-based control of swarms of vehicles. *Auton Robots*. 2004;17(2-3):137-162.
24. Kerr W, Spears D, Spears W, Thayer D. Two formal gas models for multi-agent sweeping and obstacle avoidance. In: *Formal Approaches to Agent-Based Systems*. Berlin, Germany: Springer; 2005:111-130.
25. Kerr W, Spears D. Robotic simulation of gases for a surveillance task. Paper presented at: 2005 IEEE/RSJ International Conference on Intelligent Robots and Systems; 2005; Edmonton, Canada.
26. Landau LD, Sykes JB, Reid WH. *Fluid Mechanics*. Pergamon; 1987.
27. Zhao Y, Liu Y, Duan Z, Wen G. Distributed average computation for multiple time-varying signals with output measurements. *Int J Robust Nonlinear Control*. 2016;26(13):2899-2915.
28. Wang X, Zhang J, Zhang D, Shen L. Uav formation: from numerical simulation to actual flight. Paper presented at: 2015 IEEE International Conference on Information and Automation; 2015; Lijiang, China.

How to cite this article: Wang X, Wang X, Zhang D, Shen L. A liquid sphere-inspired physicomimetics approach for multiagent formation control. *Int J Robust Nonlinear Control*. 2018;1–19. https://doi.org/10.1002/rnc.4252